ac conduction in disordered solids: Comparison of effective-medium and distributed-transition-rate-response models

J. Ross Macdonald
Department of Physics and Astronomy, University of North Carolina, Chapel Hill, North Carolina 27599-3255
(Received 5 November 1993)

Dyre has proposed that in the low-temperature limit an effective medium approximation, termed the Bryksin equation here (the BEM), predicts a universal frequency dependence for the normalized small-signal ac frequency relaxation response of nonmetallic disordered solids. This response has been claimed to be practically identical to that found for an exponential distribution of transition rates (EDTR) in the particular limiting uniform-energy-barrier-distribution case, but comparison of the two responses has been inadequate so far. Although it is shown here that they can be well differentiated, the question of which or either is universal still requires further comparisons with experiment for its answer. A generalization of the limiting low-temperature BEM equation applicable for nonzero temperatures, the GBEM, is developed and used to evaluate the temperature and frequency ranges for which the BEM is still adequate. It is found that GBEM response can be well approximated by the important EDTR solution and leads to a frequency exponent with the same temperature dependence as the latter. An expression derived herein for the dc conductivity predicted by the GBEM involves $\frac{1}{3}$ of the maximum thermal activation energy (i.e., the effective percolation energy), however, rather than the energy itself. Further, unlike the BEM, the GBEM predicts the presence of an intrinsic temperature-independent high-frequency-limiting conductivity whose magnitude is evaluated. The combination of conductive- and dielectric-system response, always experimentally present for a conductive system, is evaluated for the GBEM, and in the frequency range where the GBEM and BEM are indistinguishable it leads to frequency and temperature response remarkably similar to that observed for most disordered materials. Finally, it is suggested that Dyre's macroscopic simulations of the relaxation problem do not seem fully relevant to physical situations of interest and thus should not be taken to confirm the universality of the BEM equation response. Nevertheless, the present results broaden the likely range of applicability of both the BEM and GBEM and the EDTR and suggest that one or the other may indeed be particularly appropriate for describing the frequency and temperature response of a wide variety of disordered materials.

I. INTRODUCTION AND BACKGROUND

It is interesting and potentially important whenever a new universal response law is proposed. Recently, Dyre[1,2] predicted that the low-temperature ($T \to 0$) ac conductivity relaxation response of nonmetallic disordered solids is universally described by a particular effective medium approximation (EMA), a mean-field approach, and by the "almost indistinguishable"[3] percolation path approximation (PPA), itself mathematically equivalent to a box-type hopping response model. Such a model may be associated with a specific distribution of transitions rate (DTR),[4-11] one with all free-energy barriers equally likely. Dyre[1,2] carried out extensive Monte Carlo tests of these low-temperature universality predictions for two and three dimensions and concluded that the universality was indeed confirmed.

Dyre's EMA universality hypothesis is an appealing one, particularly because the general EMA is exact in the limits of both high and low concentrations of defects and provides a smooth interpolation between them.[12] It does, however, predict a somewhat incorrect value for the three-dimensional (3D) percolation threshold.[2] Useful recent reviews of diffusion and ac conductivity theories, including the EMA, appear in Refs. 2, 12, and 13.

Here some of Dyre's important findings are considered in further detail, with particular reference to the response of materials which conduct in three dimensions, the usual experimental situation. Because the specific EMA equation elevated to universality by Dyre, one apparently first derived by Bryksin[14] (called the BEM here), is only exactly applicable in the nonrealizable $T \to 0$ limit, it is important to investigate how well it, or a $T \geq 0$ generalization of it (the GBEM), applies at nonzero temperatures. In addition, since Dyre has compared only the real part of the PPA conductivity with experiment,[3,8] it is also of great importance to consider the frequency response of both the real and imaginary parts of the BEM and PPA dispersion contributions to the total complex conductivity. Further, by doing so at the most appropriate admittance response level,[7,9,15,16] one can investigate the degree to which these equations can be distinguished and the BEM possibly fitted by a more flexible DTR equation, the exponential distribution-of-transitions-rate (EDTR) model.[5,6,9,11,15] It is also important to examine the appropriateness of Dyre's Monte Carlo simulation results for conclusively verifying his universality hypothesis. These various matters, including the effect of the dielectric response of the material, are discussed in the following sections. Since various aspects of immittance spectroscopy[7,15,17] and the several kinds of conductive and/or dielectric relaxation possible are highly relevant to the

present work, they are briefly summarized in Appendix A, while model equations, specific definitions, and other relevant results are presented in Appendix B.

II. NUMERICAL RESULTS AND COMPARISONS FOR $T \rightarrow 0$

A. Comparisons at admittance and complex modulus levels

Since it is convenient in theoretical analysis to deal with normalized quantities, in the present conductive-system situation we shall normalize $Y(\omega)$ with $Y'(0) \equiv G_0$ to obtain $Y_N(\omega) \equiv Y(\omega)/G_0$ and also normalize the angular frequency by an appropriate relaxation time τ_X. Thus let $\Omega_X \equiv \omega\tau_X$. Then the normalized admittance equals the normalized complex conductivity $\sigma_N(\Omega_X)$, and for simplicity we shall define the normalized complex capacitance to be the same as the normalized complex dielectric constant, here defined as $C_N \equiv \epsilon_N \equiv Y_N/(i\Omega_X) = 1/M_N$, where M_N is the normalized complex modulus. There are four relaxation-response equations, derived and discussed in Appendix B, with which we shall be concerned. For the $T \rightarrow 0$ limiting situation, they are the BEM [see Eqs. (B22) and (B23)] and the EDTR box-distribution equation: the EDTR_1 [Eq. (B8)] (equivalent to the PPA when $R_{b\infty}$ is taken zero), that obtained with $\phi = 1$ in Eq. (B4). For the $T > 0$ situation, they are the GBEM of Eq. (B21) and EDTR response with arbitrary ϕ [Eq. (B8)].

Figure 1 shows a comparison between accurate BEM data and EDTR_1 predictions for Y_{bN} and $\Delta_G Y'_{bN} \equiv Y'_{bN} - Y'_{bN}(0) = Y'_{bN} - 1$ (see Appendix A). The frequency variable here is that for the EMA equation, $\Omega_E \equiv \omega\tau_E$, as discussed in Appendix B. Such log-log admittance-level comparisons have been presented earlier by Dyre for Y_{bN} over a narrower frequency range[2,3] using a frequency scaling factor Λ of 2 [see Appendix B and Eq. (B9) for further discussion of this choice]. For experimental data, however, the appropriate value of Λ would be unknown and would have to obtained by data fitting.

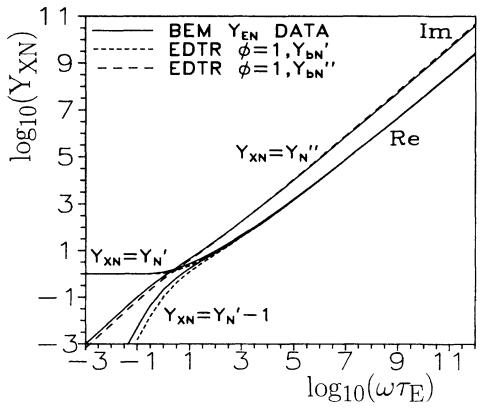

FIG. 1. Comparison of the predictions of the Bryksin effective medium (BEM) equation with those obtained by complex nonlinear fitting of the single-exponential distribution of transition rates box model ($\phi = 1$), the EDTR_1, at the normalized admittance or complex conductivity level. The normalized frequency variable $\Omega_E \equiv \omega\tau_E$ is that for the effective medium equation.

Such a fitting approach is followed here by using complex nonlinear least-squares (CNLS) fitting of both the real and imaginary parts of the box model to BEM data. The actual fitting was carried out using the LEVM CNLS program[9,18,19] with the scaling factor taken as a free fitting parameter. No $R_{b\infty N}$ factor was needed in the fitting equation (B8). The result of the fit was $\Lambda \simeq 1.35|0.02$, where the notation $A|B$ indicates a fit estimate A and its estimated relative standard deviation B. This choice leads to appreciably closer agreement between the predictions of the two equations than that found by Dyre for $\Omega_E > 1$ and to somewhat worse agreement in the $\Omega_E \leq 1$ region. But the latter region is one where comparisons with experimental data are less reliable because of the need for uncertain G_X and C_X subtractions (see Appendix A). Incidentally, the $Y'_{bN} - 1$ curve in Fig. 1 was not obtained by a new CNLS fit to $Y_{EN} - 1$ data, which would show closer agreement than that here.

In the past, most comparisons between analytic relaxation equations and between such equations and measured data have been similar to Fig. 1 in that they involved log-log plots of the real part of conductivity or admittance and usually did not even include imaginary-part comparisons.[2,3,8,10,13,20] As pointed out earlier,[2,3,9,13] it is unwise, however, to base detailed comparisons solely on such a log-log type of presentation, especially when it is apparently close to a straight line of appreciable slope. Figure 1 and Dyre's recent work[2,3] indicate, however, that even including imaginary-part comparisons as well here yields such close apparent agreement for both real and imaginary BEM and EDTR_1 predictions that one would not usually expect to be able to decide, on the basis of log-log plots of fitting results, which one yielded better agreement with actual data containing errors.

Dyre[3,8] has compared only the Y'_N predictions of the EDTR_1 with data for many materials by adjusting scaling factors, but has not presented direct fitting results of actual data to the BEM. Results were presented only as low-resolution log-log plots, and even so they showed very appreciable scatter. The agreement found was taken[2] as evidence for the universality of the BEM. Further, may of the measurements compared were for materials at temperatures near or above room temperature (one was at 873 K), not necessarily representative of $T \rightarrow 0$ response.

Much actual admittance data for solids shows approximate log-log slopes (hereafter referred to as just slopes) of Y' which fall in the range from 0.7 to nearly unity.[16,20] When the ac frequency response appears to include an appreciable region of constant slope near unity in a log-log plot, as do the results of Fig. 1, it is much more appropriate to consider it at a level which removes most of the rapidly varying parts of the response and thus reduces the range of variation, rather than to work only with log-log presentations of conductivity. For a conductive-system response associated with a box distribution of activation energies, it has been shown that the modulus level is particularly useful,[9] provided that C_X

effects are subtracted at the Y level before transforming to the M level. But transformation to obtain a complex modulus $M(\omega)$ response from results at a different immittance level requires measurements of both real and imaginary parts of the response at the other immittance level.

Figure 2 shows the data and fits of Fig. 1 transformed to the M level. In addition, the general EDTR equation was used as a fitting model. Fitting led to best-fit Λ estimates of 1.25|0.03 for the $EDTR_1$ and 1.54|0.03 for the EDTR. In the latter case, both Λ and ϕ were free parameters. The appreciable differences between these estimates, and between them and the Y-level fitting estimate, are indications that the EDTR model is not closely identical to the BEM equation and data. The Fig. 2 results further make it quite clear that EDTR and BEM responses can be very well distinguished at the M level, raising the question of whether the BEM is universal and the $EDTR_1$ is not or vice versa. Certainly, CNLS fitting of these equations to reasonably accurate experimental data should allow one to make a meaningful choice between them, at least for the particular data involved. Further, comparison of the Figs. 1 and 2 results provides a literally graphic illustration of the power of a log-log presentation to obscure real differences.

In order to allow convenient fitting of the BEM equation to actual data, it is useful to have available analytical expressions for the BEM frequency response. An ingenious analytical approximation has been presented by Dyre,[2] and its predictions at the M level are included in Fig. 2. Unfortunately, it is clear that it is not sufficiently accurate to be particularly useful for this purpose. A much more accurate approximation for the BEM response has been derived by the present author and yields results graphically indistinguishable from the accurate BEM response of Fig. 2. In fact, its maximum relative error over the entire range of $0<\Omega_E<\infty$ is only 0.066%, and its estimated standard deviation of the relative fit residuals is only 0.0017. It is thus well suited for fitting data to BEM predictions, and it will be incorporated as an available model in the forthcoming next version of LEVM.

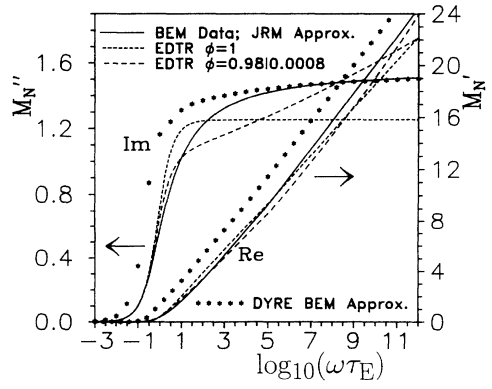

FIG. 2. Results of fitting of the EDTR-model modulus-level response M_{bN}, with $\phi=1$ and with ϕ free to vary, to BEM data, M_{EN}. In addition, results of an approximation to the BEM response derived by Dyre and results of one derived by the author (J.R.M.) are included.

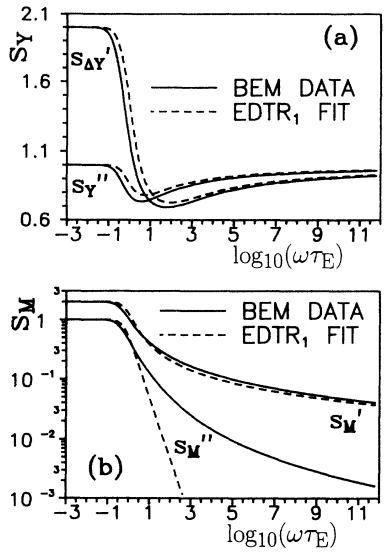

FIG. 3. (a) Slopes of the log-log plots of the BEM ($Y_{EN}'-1$) and Y_{EN}'' frequency responses vs the logarithm of normalized frequency compared with the slopes of the best-fit $EDTR_1$ response. (b) Same as above, but for complex modulus response and fit results.

Since Bryksin's first presentation of equations for the large-Ω_E limiting slopes[14] s_{EY}' and s_{EY}'' of the BEM log-log admittance plots, there have been many independent discussions of these slopes,[2,3,8,13,21] and much has been made of the fact that the slopes approach unity only logarithmically as $\Omega_E\to\infty$. In particular, Dyre[2] has shown that both the BEM and $EDTR_1$ yield identical limiting behavior in this range. Heptic spline fitting[22] of BEM data has been employed here to calculate the appropriate slopes at the admittance and modulus levels, and the results appear in Fig. 3. They indeed show how the BEM and $EDTR_1$ slopes approach each other at very large Ω_E. Some slope data for metal-cluster compounds show behavior in qualitative agreement with that here.[13] But things are different at the M level, as shown by the curves in Fig. 3(b). We see that s_{bM}'' approaches zero very rapidly, quite differently than does s_{EM}'', and that the s_{XM}' curves both exhibit simpler logarithmic limiting behavior. It is clear that for a conducting system, presentation of slopes at the M level yields more resolution and is more diagnostic than comparison at the Y level.

B. Complex dielectric constant level and probability distributions

In the present conductive-system situation, all true dielectric effects have been omitted or subtracted out. But one can still form the dielectric increment $\Delta\epsilon$ arising from the conductive-system dispersion, as discussed in Appendix A. It is of some interest to do so here because if it were not known that the dispersion was entirely conductive even when it actual was, one might subtract out the effect of a dc conductance, analyze the results at the

dielectric level, and identify them with real dielectric effects,[20,23] not an uncommon misinterpretation.

Results of calculating the normalized dielectric increment $\Delta\epsilon_N$ are presented in Fig. 4. Figures 4(a) and 4(b) are direct and log-log complex-dielectric-plane plots, respectively, and Fig. 4(c) shows the log-log frequency response behavior. Here the BEM response is compared with that of two different CNLS fits. One such fit is just the transformed fit results of the $EDTR_1$ model of Figs. 1 and 2, while the other was generated by fitting the transformed BEM response directly at the ϵ level using the EDTR model with the parameter ϕ free to vary. For this fit, the estimates of Λ and ϕ obtained were $\Lambda=3.9|0.08$ and $\phi=0.189|0.016$. The negative of this value closely equals the slope of the dashed straight lines in Fig. 4(c), since for $\phi<0.5$, $-\phi$ is a good measure of the high-frequency limiting slope of the EDTR response at the dielectric level.[7,15]

It is evident that the two different fit results are quite different, with the first one, that with $\phi=1$, fitting the high-frequency region of the data much better and the other yielding better results at low relative frequencies. But both fits are so poor that one could readily distinguish between true BEM response data and the EDTR model, at this level, which is another instance of differences between these responses which are largely obscured at the Y level. Finally, because the curves of Fig. 4(a) are all qualitatively similar to the predictions of the Davidson-Cole response function,[24] often used for fitting true dielectric response data, their incorrect identification with such a response is made more likely.[9]

There is another way that relaxation data can be fitted without preconceptions concerning a specific fitting model. Using LEVM, one can fit data by CNLS to an arbitrary distribution of relaxation times.[16] The model is made up of N simple Debye responses: At the dielectric-system ϵ level, they may be thought of as N branches in parallel, each involving a resistor and capacitor in series, while at the conductive-system M level they consist of N parallel resistor-capacitor pairs in series. The process optimizes the fit by adjusting the strength of each pair p_i and its relaxation time τ_i to achieve a minimum sum of squared relative residuals. For error-free data of the present kind, fitting can be made arbitrarily good just by increasing N. In this fashion, a possibly continuous DRT is approximated by a discrete distribution, with the sum over N of the p_i's normalized to unity.

Here sufficient accuracy is achieved by the choice $N=14$, requiring the determination of 28 fitting parameters. Figure 5 shows the results of applying this technique to the present BEM data and EDTR-fit results. With the proportional weighting[18] used here, the results of fitting at the ϵ or Y level are the same, as are those for the Z and M levels. In the bottom part of the figure, lines have been included to guide the eye, although only the points themselves are significant. For the ϵ-level fitting, Y data were first transformed to $\Delta\epsilon$ data. No C_∞ subtractions were needed for M-level fitting, since no dielectric contributions are present in these synthetic data. The irregularities at the low- and high-τ extremes arise from the finite range of the data, but we nevertheless see regular behavior over ten decades or so for each of the fits. Further information on DRT's for different immittance levels may be found in Refs. 26–28.

Figure 5, being a log-log plot, actually shows the normalized distribution of activation energies, $F(E)$, since $\ln(\tau/\tau_E)$ is proportional to E. We see that the points of the dielectric-level, EDTR-fit curve, with $\phi\simeq0.189$, lie on a straight line with exactly this value for the slope, $d[\ln(p_{\epsilon i})]/d[\ln(\tau_i/\tau_E)]$, in complete accord with expectations.[15] But note that the $p_{\epsilon i}$ points for the BEM and

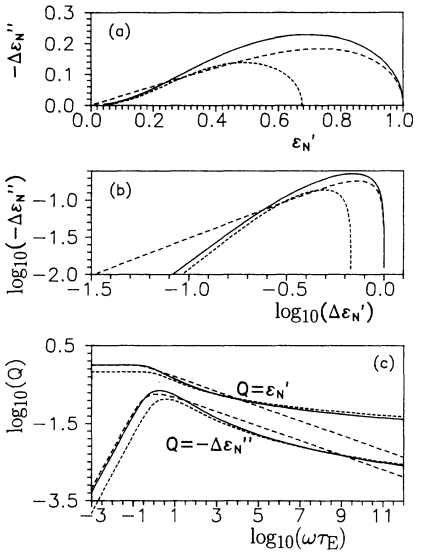

FIG. 4. (a) Complex dielectric plane plot of the conducting-system dielectric increment for the BEM response (solid line), $EDTR_1$ fitting at the Y level and transformation to the ϵ level (short-dashed line), and EDTR fitting directly at the ϵ level with ϕ free (long-dashed line). (b) Same as (a), but log-log plot to show constant limiting slopes. (c) The frequency dependences of the $\Delta\epsilon_N'$ and $-\Delta\epsilon_N''$ responses of (a) and (b) shown as log-log plots.

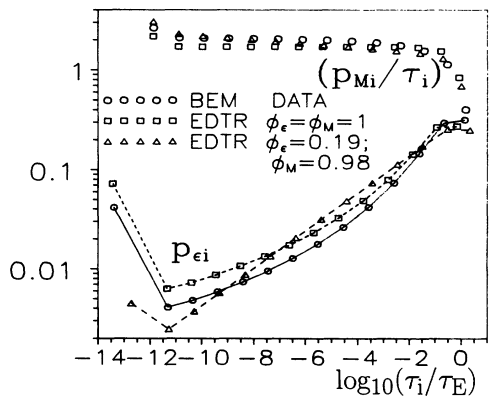

FIG. 5. Discrete-probability-distribution strength values p_i for the conducting-system response p_{Mi} and for the dielectric-level response of the conducting system, $p_{\epsilon i}$. The lines joining the points are included solely to guide the eye. The distribution behavior is shown for the BEM data and for data obtained from $EDTR_1$ and EDTR CNLS fits to the BEM response.

the box-distribution-fit results lie on a curve when the end points are eliminated. This behavior is associated with the curved responses shown in Fig. 4(c) and again is to be expected. Over the nearly eight decades between $y \equiv \ln(\tau_i/\tau_E) = -11.3$ to -3.6, the BEM p_i response is very closely given by $p_i \simeq (\tau_i/\tau_E)^{-1/g(y)}$, with $g(y)$ linear or quadratic in y.

For a conductive-system box distribution, only at the M level does a constant (actually zero) slope appear, that of the M''_{bN} curve of Fig. 2. The top part of Fig. 5 reflects just this behavior in the appropriate distribution function. The slope is there essentially zero because the EDTR function for the conductive-system response is a constant for the flat-top box distribution.

Dyre[2] states that the importance of the BEM, his Eq. (40), "lies in the fact that the equation is universal, completely independent of the activation energy probability distribution." Indeed, his simulation results, discussed below in Sec. III A, all approach a kind of BEM response as $T \to 0$ for all distributions considered. The present results show, nevertheless, that a specific activation energy distribution is clearly associated with the BEM. Only for this particular distribution does one obtain a characteristic BEM frequency response. Thus again the question of universality seems to remain moot.

III. NUMERICAL RESULTS AND COMPARISONS FOR $T>0$

A. Simulation results and comparisons

Dyre[1,2] has carried out interesting and extensive computer simulations of a two- or three-dimensional lattice of admittances for a range of β values. For $D=3$, a $50\times50\times50$ lattice was used, with the value of each elemental admittance link made up of a resistor and a capacitance in parallel. All capacitances were taken identical and the thermally activated resistor values were each determined by an activation energy determined randomly from a particular probability distribution (including the box distribution). This activation involved βE, not $\beta E/3 \equiv \beta E_c$, where E_c is a percolation energy (see Sec. III B). The simulations were carried out starting with the Maxwell equations to calculate an overall quasiadmittance, but with the $i\omega$ terms arising from the small-signal ac factor $\exp(i\omega t)$ replaced by just ω in the simulation equations.

As Dyre[1] points out, this is possible when the purpose is to compare simulation results to an analytic function. Although this decision probably greatly simplified the simulation, for consistency it required that the large-β results be compared not with the predictions of the BEM of Eq. (B23), but with that equation with $i\Omega_E$ replaced by Ω_E; call it BEMR. As a consequence, neither the BEMR nor the simulation led to both real and imaginary values of $Y_N(\Omega_E)$, but to a single real quantity, say, $Y_{RN}(\Omega_E)$, identified as a conductivity.[2] Dyre[1,2] indeed found that as β increased toward large values, the normalized simulation results approached the BEMR prediction, although the largest β value for which simulation results were found, 60, was insufficient for the 3D simulation results to approach those of the BEMR very closely. Nevertheless, Dyre concluded that the simulation results verified the universality of the BEM frequency dependence at low temperatures.

What is the meaning of these intriguing results, and do they indeed justify Dyre's conclusion? To begin to answer these equations, it is useful to compare BEMR and BEM predictions. First, it is clear that Dyre's Y_{RN} simulation results,[2] which are given for a range of values of β rather than involving the $x_s \equiv \beta E_H$ of the present work (see Appendix B), are qualitatively similar to the Y'_{EN} results of Fig. 1 for small Ω. They then approach a constant saturation value at large Ω and intermediate values of β, and they finally approach the Fig. 1 Y''_{EN} curve for sufficiently large values of Ω_E and β. Thus it is worthwhile to compare $Y_{RN}-1$ with Y''_{EN} and with the modulus function $[(Y'_{EN}-1)^2+(Y''_{EN})^2]^{1/2}$. Calculated percentage differences for these comparisons are presented in Fig. 6, which indeed shows the approach of the BEMR Y_{RN} predictions to Y''_{EN} as $\Omega_E \to \infty$, but also indicates that the modulus function is mostly an appreciably better approximation to Y_{RN} than is Y''_{EN}.

Since Y_{RN} is clearly some complicated, unknown function of both Y'_{EN} and Y''_{EN} and does not yield separate real and imaginary parts of an admittance, it seems inappropriate to identify it as one, and it does not allow the calculation of immittances at other levels. As we have seen, comparison of conductive-system Y'_N predictions plotted in log-log fashion is not particularly diagnostic, and comparison at the M level, where one usually need not make a logarithmic transformation, can allow far better discrimination. Since the BEMR and corresponding simulation results do not yield results which can be compared with actual immittances, either real-only or both real and imaginary parts, it seems premature to form definite conclusions about the physical relaxation response from such an approach.

This conclusion, plus the earlier analysis and comparisons in the present work, suggests that although the

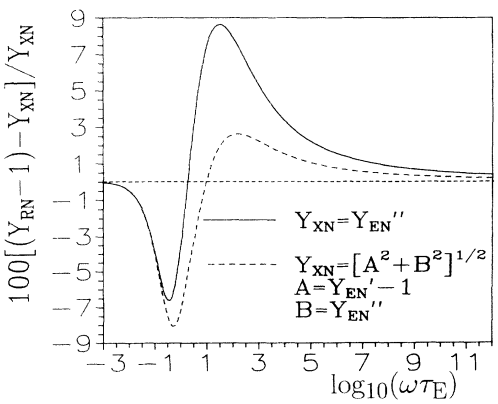

FIG. 6. Comparison between the $T \to 0$ Y_{RN} response, obtained by solving Eq. (B16) with $i\Omega_E$ replaced by Ω_E as proposed by Dyre (Ref. 2) for comparison with his simulation results, with two different BEM quantities, where here Y_{EN} is the solution at the Y level of the unmodified Eq. (B16).

BEM is a fascinating response function, its universality for temperatures where GBEM and BEM predictions are negligibly different remains still unproven. Clearly, a comparison of actual disordered-material relaxation-response data with BEM (and perhaps EDTR) frequency-response predictions for a range of temperatures is badly needed and is now readily possible with the inclusion of the BEM as a fitting function in the LEVM program. Even if the frequency response is indeed well fitted, it would be crucial to investigate if the estimated value of $R_{E\infty}$ found from the fitting satisfies Eq. (B20), if estimated values of R_{E0} and τ_E are activated as in Eqs. (B25) and (B26) and agree with these theoretical values, and if the $E_H/3$ values obtained from these equations are consistent with activation energies for the material determined by other means.

B. GBEM response

Thus far, we have followed Dyre's approach and primarily considered only $T\rightarrow 0$ forms of the effective medium and EDTR equations, with the expectation[1-3] that they will nevertheless be useful over some nonzero range of temperatures. This assumption needs to be tested, particularly because it has not been adequately examined so far by fitting of real and imaginary relaxation frequency responses to theoretical predictions. Since the EMA is itself an approximate approach, the BEM equation must be corresponding approximate, but nevertheless it and its $T\geq 0$ generalization, the GBEM of Eq. (B21), may possibly be sufficiently accurate to yield useful descriptions of some or much conductive-system relaxation behavior.

The derivation of the GBEM in Appendix B is based on an EMA solution of the random, free-barrier model with a uniform distribution of barriers (the flat-top box distribution). Since the EDTR equation may also be derived from the random-free-barrier model with either a uniform or an exponential distribution, it is indeed plausible to consider a specific EMA solution for a flat-top box distribution. Further, the GBEM leads to a response of the same general character as those found earlier by Bryksin[14] and by Fishchuk.[21] Even if the EMA Green's function used by Dyre,[3] on which the present GBEM solution is based, should be found to be overly approximate, the present GBEM equation should nevertheless be valuable for comparison purposes and probably even for data fitting. In the future, it would be worthwhile to compare the results of a GBEM solution involving a simple cubic lattice Green's function[25] to that obtained here, but extensive computation will be required to do so.

Little attention has been paid in the past to possible temperature-dependence differences between EDTR and BEM and GBEM responses (see Sec. III C). For $r\gg 1$, the Appendix B results show that the EDTR_1 low-frequency-limiting resistance R_{b0} is thermally activated as $T\exp(\beta E_H)$, the corresponding relaxation time $\tau_H\equiv\Lambda\tau_E$ is thermally activated as $\exp(\beta E_H)$, the R_{E0} for the GBEM is thermally activated as $\exp(\beta E_H/3)\equiv\exp(x_s/3)\equiv r^{1/3}$, and τ_E is thermally activated as $T^{-1}\exp(\beta E_H/3)$. Here E_H is the maximum activation energy or enthalpy. Thus the EDTR_1 model assumes that a maximum value of E exists and is directly involved in the thermally activated response, while the BEM makes the same assumption but yields an activation involving the percolation energy E_c instead of E_H. Clearly, better agreement between the temperature responses of the two models is produced if the E_H in the EDTR_1 (and EDTR) is replaced by E_c, but this obscures the real differences between the models.

The factor $E_c\equiv E_H/3$ in the GBEM results is particularly significant. Dyre[1,2] gave no explicit expression for R_{E0} or for his $\sigma(0)$ for $T>0$ conditions and did not consider the temperature response explicitly, but did state that for his simulation results $\sigma(0)\propto\exp(-\beta E_c)$. Further, Fishchuk's independent box-distribution EMA solution[21] also yielded an activation with the $\frac{1}{3}$ factor present. But as Dyre[2] points out, simulations in three dimensions have shown that the link percolation threshold value is 0.2488 rather than $\frac{1}{3}$. In view of the approximations inherent in the EMA approach, it seems reasonable to replace the effective E_c arising from the GBEM calculation by $E_H/4$. To do so, one would just replace all $x_s/3$ terms in the present work by $x_s/4$. This has not been done in the following, but should certainly be considered when comparing theory and experiment for a range of temperatures.

An important difference between the BEM and GBEM equations is that for $T>0$ the latter involves a nonzero high-frequency limiting resistance $R_{E\infty}$, whose value is, from Eq. (B27), just $\zeta\equiv\tau_a/C_c$, equal to 1 Ω for $\tau_a=1$ ps, and a value of C_c, the capacitance of the empty measuring cell, of 1 pF. Unlike any R_∞ present in an EDTR fit, $R_{E\infty}$ is an intrinsic part of the response and is thus not a free parameter.

Figure 7 shows how the GBEM response deviates from that of the BEM for several values of x_s at the (a) Y level and at the (b) M level. The plateau values of Y'_{EN} apparent in Fig. 7(a) have limiting values of just $(R_{E\infty N})^{-1}$, allowing accurate estimation of $R_{E\infty}$ from experimental results, which show activated barrier behavior. Thus $R_{E\infty}$ plays an important role in the high-frequency response when $T>0$. In contrast, the high-frequency-limiting values of the M'_{EN} plateaus in Fig. 7(b) are equal to x_s. The unnormalized plateau value is then just $9/\xi\simeq 35.6$ for the GBEM model, a value which should certainly be tested against experimental results since the value of $\xi\simeq 0.253$ is calculated under the assumption that a simple cubic lattice is appropriate.

Define the point where $Y'_{EN}=Y''_{EN}$ in Fig. 7(a) and $M'_{EN}=M''_{EN}$ in Fig. 7(b) as the normalized crossover frequency Ω_C; it is approximately given by $0.7r^{1/3}$. Then the corresponding unnormalized crossover frequency f_C is about $0.6/(x_s\tau_a)$, proportional to temperature. Examination of Fig. 7(a) shows that at least on a log-log plot there is negligible observable difference between GBEM and BEM predictions for $\Omega\leq 0.1\Omega_C$, corresponding to an actual frequency of less than about $0.001/\tau_a$ Hz for $x_s=60$. For $\tau_a=10^{-12}$ s, discrimination would then be difficult for $f<10^9$ Hz, a frequency higher than used for most measurements in the present field. Thus it is not surprising that such measurements usually show no pla-

teau in Y'. To observe such behavior, one would need to measure to very high frequencies at low temperatures. A few measurements[29–31] do indeed extend to 10^{12} Hz or so, the optical phonon frequency region, and show a plateau in σ' in that neighborhood. Further, Bryksin's original analysis[14] predicted a plateau in the optical-phonon frequency region, as did related work of Fishchuk,[21] both consistent with the present results.

Dashed lines in Fig. 7 show EDTR fits to the GBEM data for the choice $x_s=40$. Although results at the Y level are virtually indistinguishable from the data, they are sufficiently different at the M level that even in a log-log plot some differences can be resolved. The line of short dashes in Fig. 7(b) was calculated by removing the EDTR fit estimate of the normalized high-frequency-limiting resistance $R_{E\infty N}$ from the EDTR M_N''-fit results; it shows that the rapid rise in the M_{EN}'' curves at high frequency is entirely associated with the presence of an intrinsic nonzero limiting resistance. This high-frequency-limiting behavior of M_{EN}'' for $T>0$, a rise proportional to Ω, also

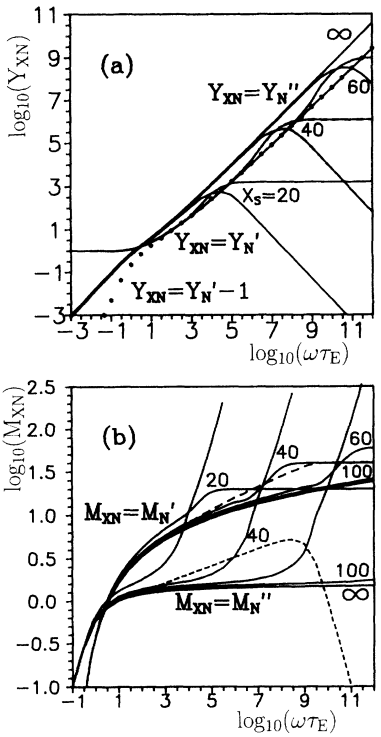

FIG. 7. (a) Log-log plot of the Y_{EN} response (solid lines and asterisks) calculated using the GBEM for $x_s\equiv\beta E_H$ values of 20, 40, 60, and ∞. For $E_H=1$ eV, these values correspond to temperatures of about 580, 290, 193, and 0 K, respectively. The dashed lines, virtually indistinguishable here, are EDTR-fit results to the $x_s=40Y_{EN}$ data. (b) M_{EN} log-log response curves for five values of x_s (solid lines), for a EDTR fit at the M level of the $x_s=40M_{EN}$ data (long-dashed line), and for the same fit with the effects of the estimated value of $R_{E\infty N}$ removed (short-dashed line). The fit estimates were $\Lambda=1.74|0.03$, $x_s=41.0|0.03$, $\phi=0.914|0.004$, and $R_{E\infty N}=8.27\times10^{-7}|0.03$. For comparison, the actual value of $R_{E\infty N}$ at $x_s=40$ is about 8.098×10^{-7}.

leads to the peak and subsequent decay in the corresponding Y_{EN}'' curves of Fig. 7(a), a response which also disappears when $T=0$ and $R_{E\infty}$ is itself zero.

Fits of the EDTR to GBEM data for $x_s=40$, 60, and 100 lead to ϕ estimates which may themselves then be fitted to a linear expression in $1/x_s$. The result found is $\phi\simeq1.02-4.28/x_s$, in full agreement, within its uncertainties, with the temperature dependence of the ϕ parameter which is intrinsic to a conductive-system EDTR response[6,7,15] (class I): $\phi=1-\eta/\beta$, where η is a temperature-independent constant. Thus, although there is no ϕ in the GBEM equation, its response can clearly approximately mimic that of the EDTR right down to the temperature dependence of the EDTR ϕ parameter, at least for $\phi\leq1$. Since the EDTR has been found to fit well an extensive amount of experimental data, this suggests that the GBEM may also be able to do so. Surprisingly and importantly, these results indicate that a response function based on a random-free-barrier model with equally likely barrier energies can nevertheless simulate the response following from an exponential distribution of barrier energies, at least over a limited low-temperature range.

Figure 7(b) shows large differences between GBEM and BEM predictions for M_{EN}' and M_{EN}'' at frequencies much less than Ω_C. For $x_s=40$, for example, appreciable differences appear for Ω_E values as small as 100. For $\tau_a=10^{-12}$ s, this value corresponds to an actual minimum frequency of discrimination, f_d, of about 3.8×10^6 Hz, one well within the range of some of the σ' data compared by Dyre[3] to EDTR_1 box-distribution predictions. For $x_s=60$, about 100 K below room temperature for $E_H=1$ eV, f_d is only about 3×10^5 Hz. Dyre[2] has stated that the capacitance currents associated with ϵ_∞ are negligible at low temperatures and moderate frequencies. Here, where we use C_X (or ϵ_X) rather than C_∞ (see Appendix A), the neglect of the effect of C_X, especially in regard to its influence on measured M'' data, is by no means warranted, particularly since its effects occur at lower frequencies the lower the temperature.

C. Effect of C_X: experimental analysis

The reasons the strong rise in M'' and the corresponding peak in Y'' at large frequencies, both associated with a nonzero R_∞ value, are generally not evident in actual conducting-system data[32,33] is because C_X is not usually estimated and subtracted from the data before calculating and plotting data at the M and Y levels. Without such subtraction, one is not examining the actual conducting-system relaxation response, but that response in parallel with the capacitance C_X. Although C_X has no effect on $Y'(\omega)$, the quantity usually plotted, as we shall see it has a great effect on $M''(\omega)$.

When one wishes to compare results such as those in Fig. 7 with experiment, one must either estimate and subtract the effect of C_X or add its effects to those above. We shall illustrate the effects of both choices here. Figure 8(a) shows M_N'' results for $x_s=40$ obtained by first adding the term $i\Omega_E C_{XN}$ to Y_{EN} or Y_{bN} data. Here

$C_{XN} \equiv \epsilon_{XN} \equiv C_X / C_{E0}$, where C_{E0} is the low-frequency-limiting conductive-system EMA capacitance increment given in Eq. (B18). The solid curve for $C_{XN}=0$ involves directly calculated GBEM points, while the other solid-line curves were formed by starting from the EDTR fit to that data. We see that a nonzero value of C_{XN} can make a tremendous difference in the response and that it can entirely eliminate the intrinsic rise in M''_{EN} of Fig. 7(b) and leads to a peak for M''_N, just as usually observed experimentally. The peaks in the low-frequency region of the response occur approximately at $\Omega_L = 0.34 + 0.66 C_{XN}^{-1}$ for $0.5 < C_{XN} < 20$. The figure also shows that there are small high-frequency peaks which occur near the crossover frequency of Fig. 7. For most situations, they will occur at actual frequencies beyond the available measurement range. Incidentally, when points in this second peak region are calculated directly from the GBEM model with high frequency-resolution, an apparent discontinuity in the slope appears in this region, perhaps a reflection of a discontinuity of this type in the Green's function.[25]

The two curves defined by open symbols in Fig. 8(a)

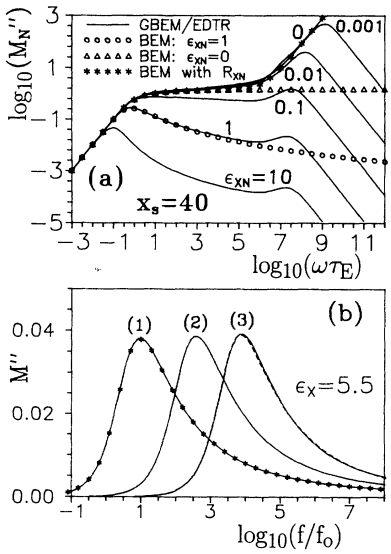

FIG. 8. (a) Normalized modulus-level overall log-log response of M''_{EN} vs Ω for $x_s=40$ when a normalized capacitance $C_{XN} \equiv \epsilon_{XN} \equiv C_X / C_{E0}$ is added to the GBEM conductive-system response to account for intrinsic dielectric contributions. The open-symbol curves show similar response using the BEM rather than the GBEM. The asterisk points were calculated with $\epsilon_{XN}=0$ using the BEM with the $x_s=40$ GBEM high-frequency limiting resistance $R_{XN}=R_{E\infty N}$ added to it at the impedance level. (b) Unnormalized M'' vs $\log_{10}(f/f_0)$ curves for three values of x_s and $\epsilon_X \equiv C_X/C_c = 5.5$. Here $f_0 \equiv 1$ Hz. The curves marked (1), (2), and (3) were calculated for temperatures of 333.3, 344.6, and 353.9 K, respectively. The points marked with asterisks on the left curve were calculated using the BEM rather than the GBEM, but with GBEM limiting parameter values employed for transforming from normalized to unnormalized response. The dashed line at (3) is a result of a EDTR CNLS fitting of the unnormalized real and imaginary GBEM response with $\epsilon_X = 5.5$ effects included.

were calculated as above by using the BEM rather than the GBEM. They thus show clearly where the two kinds of response begin to diverge. Finally, the asterisk points were calculated for $\epsilon_{XN}=0$ using the BEM with $R_{E\infty N}$ added to it, a simple approximation to the GBEM. It is clear that for x_s near 40 and $C_{XN} \geq 0$ the approximation could well be sufficiently close over the measured frequency range that one could not readily distinguish which of the two would better describe reasonably good experimental data. An even simpler approach would be to use the EDTR [Eq. (B7)], a built-in response function in the LEVM program, to fit both experimental data and the related GBEM response. Certainly, a detailed comparison of EDTR fits to data with fits of the same data using the BEM or GBEM is much needed to resolve which is the most appropriate and perhaps to help settle the question of the possible universality of the BEM.

To give a flavor of such fitting, I have considered some of the experimental[32] $M''(f)$ results for $0.4Ca(NO_3)_2$-$0.6KNO_3$, a glass-forming molten salt, at $T=333.2$, 344.6, and 353.9 K, all in the liquid range. Although these 1974 data were not available, enough results were presented[32] to allow semiquantitative comparisons. To do so, I used the published value of $C_c \simeq 0.9$ pF and determined τ_a and E_c from the published values of σ_0 in this temperature range where Arrhenius thermal activation behavior is closely followed. The results were $\tau_a \simeq 1.3 \times 10^{-53}$ s, $E_c \simeq 3.3$ eV, and $x_c \simeq 115$, 111, and 108 for the above temperatures, respectively. The only free parameter is then ϵ_X. Its value was selected to both to give rough agreement with the total published value of $\epsilon'(0) = \epsilon_{E0} + \epsilon_X$ and to make peak frequencies agree with those observed. If there is no dielectric dispersion in the present frequency range, then $\epsilon_X = \epsilon_{m0}$, where ϵ_{m0} is the low-frequency-limiting value of the true dielectric constant of the material, for which a value of 5.5 is perhaps not unreasonable. The frequency-response results are shown in Fig. 8(b), where (1), (2), and (3) identify the above temperature choices, respectively. For $\epsilon_X = 5.5$, $\epsilon_{XN} \simeq 0.57$ for curve (1). Results for $x_s = 4x_c$ are the same as those found here with $3x_c$ provided a consistent value of τ_a, equal to two-thirds of that above, is used.

The origins of the asterisk points on the $T=333.3$ K curve (1) and the dashed curve at $T=353.9$ K (3) are explained in the caption of Fig. 8. They show that for conditions such as these, one can expect that the BEM will be a quite adequate approximation to the GBEM and that the EDTR can approximate either one within usual experimental accuracy. Thus one can use the LEVM CNLS program to fit experimental data directly choosing the JRM approximation to the BEM if available or using the EDTR response function. But GBEM values of R_{E0}, τ_E, and $R_{E\infty}$ are needed to unnormalize the BEM and/or to compare with fitting estimates from the EDTR fit.

In the present instance, the range of the curve-(3) data is limited and EDTR fitting cannot yield estimates of x_c or R_{E_∞}. The fit led to an estimate of R_{E0} about 11% too high and to an ϵ_X estimate of 3 rather than 5.5. Nevertheless, the figure shows that a close fit was obtained. Only if the effect of ϵ_X was subtracted from the data be-

fore fitting was it possible to obtain a ϕ estimate consistent with the usual EDTR class-I temperature dependence. Better parameter estimates may be expected when fitting the BEM to real or synthetic data for which the BEM model is appropriate.

Incidentally, although $M'(f)$ predictions and comparison with experimental results are not shown graphically here, GBEM with $\epsilon_X = 5.5$ predictions led to extremely similar behavior, with a saturation value of M' at the highest frequencies of ϵ_X^{-1}, slightly larger than the experimental value. That value yields $\epsilon_X \simeq 7.35$.

The solid curves of Fig. 8(b) are very similar to the comparable experimental ones[32] except in one respect: the M'' peak values increase here slightly with increasing temperature, while the experimental ones decrease faster than proportional with increasing temperature. Such a decrease is often found, although temperature independence is also common.[33] The only way the present work can accommodate such results is for ϵ_X itself to increase with temperature, but the reason for such behavior is unknown. Even without such an adjustment, the present results seem to agree with the plotted data[32] much closer than a factor of 2.

The value of τ_a found from the fitting is very much smaller than the 0.01–1-ps range one might expect for optical phonons. Hopping-percolation theories usually lead to estimates of $\sigma'(0)$ that are eight to ten decades too high (e.g., see Ref. 13, p. 37), requiring a value of τ_a here of the order of 10^{-20} s, but the present estimate, which follows directly from experiment, is far smaller. It was shown in Ref. 32, however, that at temperatures appreciably higher than 350 K, E_c beings to decrease strongly with temperature. Thus the present τ_a value is not applicable at these high temperatures, and the present approach is then no longer appropriate.

The present work suggests, nevertheless, that a CNLS comparison between good data and the EDTR and BEM models for an appreciable frequency range and for several different temperatures should allow one to decide which of the two theoretical models is the more appropriate, particularly if ϵ_X can be well estimated. Further, the semiquantitative agreement between BEM temperature predictions and experiment discussed above suggests that these theoretical results may be particularly valuable for fitting of experimental data with either model. Finally, it is clearly extremely important to distinguish between conductive-system and dielectric-system effects and to avoid treating conductive-response dielectric increments as an unrecognized part of dielectric response.

ACKNOWLEDGMENT

The valuable comments and suggestions of Professor W. J. Thompson are much appreciated.

APPENDIX: IMMITTANCE LEVELS AND CONDUCTIVE AND DIELECTRIC RESPONSE

There are four immittance levels: admittance,

$$Y(\omega) = Y'(\omega) + iY''(\omega) \equiv G(\omega) + i\omega C'(\omega) \ ; \qquad \text{(A1)}$$

complex dielectric constant (or complex capacitance),

$$\epsilon(\omega) = \epsilon'(\omega) - i\epsilon''(\omega) \equiv Y(\omega)/(i\omega C_c) \equiv C(\omega)/C_c \ ; \qquad \text{(A2)}$$

complex modulus,

$$M(\omega) = M'(\omega) + iM''(\omega) \equiv 1/\epsilon(\omega) \equiv i\omega C_c Z(\omega) \ ; \qquad \text{(A3)}$$

and impedance,

$$Z(\omega) = Z'(\omega) + iZ''(\omega) \equiv 1/Y(\omega) \ . \qquad \text{(A4)}$$

Here C_c is the capacitance of the empty measurement cell. Experimental measurements usually yield $Y(\omega)$ or $Z(\omega)$. Knowledge of the value of C_c allows one to convert $Y(\omega)$ and $C(\omega)$ results to complex dielectric constant ones and $Y(\omega)$ values to complex conductivity values; $\sigma(\omega) \equiv \epsilon_V Y(\omega)/C_c = \sigma'(\omega) + i\sigma''(\omega)$. Here ϵ_V is the permittivity of vacuum. For normalized, dimensionless quantities, these distinctions are unimportant.

There are three generic relaxation dispersion situations which may occur for solids in the frequency range of measurement: conductive-system dispersion associated with mobile charge carriers, dielectric-system dispersion usually arising from dipole rotation of lattice entities, and the presence of both types of dispersion within the measured frequency range.[6,13,15] Specifically, consider possible conductive dispersion from $Z'(0) \equiv R_0$ down to a high-frequency limiting value R_∞ and possible complex capacitance dispersion from $C'(0) \equiv C_0$ down to $C_\infty \equiv \epsilon_\infty C_c$, i.e., the geometrical capacitance, C_g.

When only conductive-system dispersion is present in the measured frequency range, the intrinsic dielectric-system capacitance must be frequency independent in this range and will be either C_0 or C_∞ depending, respectively, on whether the dielectric dispersion occurs at frequencies far higher than the conductive relaxation or vice versa. Define the appropriate capacitance as C_X. Then, to obtain just the dispersive part of the conductive-system response, one must subtract the effects of C_X to form[15,16]

$$\Delta_C Y \equiv Y - i\omega C_X = Y' + i(Y'' - \omega C_X) \ . \qquad \text{(A5)}$$

For the present conductive-system theoretical work, in order to agree with Dyre's results at the $\sigma(\omega)$ level, we initially assume that the effect of C_X has already been subtracted, and thus we shall not distinguish further between Y and $\Delta_C Y$ in the main text unless C_X is explicitly taken nonzero.

But even for a conductive system, it is often of interest to calculate the effective dielectric increment arising from such conduction.[16] When the effect of C_X has been removed, this increment, although defined at the complex capacitance or complex dielectric constant level, has nothing to do with dielectric processes. To obtain this increment, we must form[16]

$$\Delta_{CG} Y \equiv \Delta_C Y - G_X = (Y' - G_X) + i(Y'' - \omega C_X) \ , \qquad \text{(A6)}$$

where $G_X \equiv 1/R_X$ and R_X is then R_0 or R_∞, the choice again depending on the relative frequency ranges of the dielectric and conductive dispersions. The dielectric increment is, then,

$$\Delta\epsilon \equiv \Delta_{CG} Y/(i\omega C_c) = \Delta\epsilon' - i\Delta\epsilon'' \ , \qquad \text{(A7)}$$

where the CG subscript has been omitted for simplicity here. The real part of the complex capacitance associated with $\Delta\epsilon$ is just $C_c'(\omega)\equiv C_c\Delta\epsilon'$.

A not entirely uncommon error is to confuse the dielectric increment arising only from the conductive-system dispersion with dispersion arising from a true dielectric response (e.g., see the discussion in Ref. 16). This misinterpretation is less likely to occur if one discusses and analyzes the conductive-system response at the natural Z (or complex resistivity) and M levels and the dielectric-system response at its natural complex C (or ϵ) and Y levels.[15,16]

When one deals with experimental data, one must obtain as accurate estimates of C_X and/or R_X as possible because the above subtractions often involve regions where we must deal with small differences between two large, nearly equal quantities. Consider the determination of C_X from conductive-system experimental data when $C_X=\epsilon_\infty C_c$ over the entire measured frequency range. Since $\Delta C'(\infty)\equiv C_c\Delta\epsilon'(\infty)$ is generally zero, we can find all limiting capacitance values from $C_0\equiv C'(0)=\Delta C'(0)+C_X$ and $C_\infty\equiv C'(\infty)=C_X$. Finally, when both conductive and dielectric dispersions are present in the frequency range of measurement, it is most appropriate to estimate values of the pertinent parameters of the response, such as C_0, C_∞, R_0, and R_∞, from CNLS fitting of the full data to a model which includes both types of response. Such fitting is particularly easy to carry out with the powerful LEVM program,[18,19] and LEVM has been used for all the calculations of the present work.

APPENDIX B: SPECIFIC RESPONSE EQUATIONS

In this appendix several relaxation equations related to those used by Dyre[1-3] are discussed: one following from the assumption of an exponential distribution of transition rates, the EDTR, and the others appropriate for a uniform distribution, the EDTR$_1$, the effective-medium-approximation BEM equation, and its $T\geq 0$ generalization, the GBEM equation. Because it is natural to deal with an experimental conductive-system response at the impedance level, the quantities of interest will be expressed here as resistances and capacitances, unnormalized or normalized, rather than as resistivities and dielectric constants. Impedances and resistances will be normalized, when appropriate, with their dc limit R_0.

1. Conductive-system response: EDTR and EDTR$_1$ models

We follow earlier work for a conducting system by assuming that the local conductivity and transition rates are thermally activated with a distribution of free-energy barriers.[5-11] For simplicity, assume that the distribution is in the activation energy E (actually enthalpy) only. Then a transition rate Γ and related relaxation time τ may be expressed as

$$\Gamma/\Gamma_a\equiv(\tau/\tau_a)^{-1}=\exp(-\beta E)\ , \tag{B1}$$

where $\beta\equiv 1/k_BT$ and Γ_a is a barrier attempt frequency. Further assume that the distribution is cut off at both ends,[6,15] so that it is nonzero only for $E_L\leq E\leq E_H$. Finally, we shall make the plausible and usual assumption that the E's are temperature independent (defined as class-I behavior[15]). We can now write for the important ratio of maximum to minimum transition rates,

$$r\equiv\exp(x_s)\equiv\Gamma_H/\Gamma_L=\tau_H/\tau_L=\exp\{\beta(E_H-E_L)\}\ . \tag{B2}$$

In the present work, we follow usual practice and set $E_L=0$, and so $\Gamma_H=\Gamma_a\equiv\tau_a^{-1}$. For the box distribution, the activation energy probability distribution is then just $p(E)=1/E_H$ for $0\leq E\leq E_H$ and zero otherwise. The corresponding distribution for Γ is proportional to Γ^{-1}, and the average $\langle\Gamma\rangle$ over this distribution is readily found to be $\Gamma_H(1-r^{-1})/x_s$, equal to Γ_H for $x_s\equiv\beta E_H=0$.

It is often convenient to express a general frequency-response relaxation function $U(\Omega_X)$ as a normalized immittance,[6,11]

$$I(\Omega_X)\equiv[U(\Omega_X)-U(\infty)]/[U(0)-U_j(\infty)]\ , \tag{B3}$$

defined at the impedance level for the conductive-system response and at the complex dielectric level for dielectric-system relaxation. Thus $U(0)$ and $U(\infty)$ are R_0 and R_∞ in the former case and ϵ_0 and ϵ_∞ for the latter. The EDTR equation, also termed a single-exponential-distribution-of-activation-energies equation in past work,[7,11,15] can now be expressed as

$$I(\Omega_H)\equiv\phi[1-\exp(-\phi x_s)]^{-1}\int_0^{x_s}\frac{\exp(-\phi x)dx}{1+i\Omega_H\exp(-x)}$$

$$\equiv A(x_s,\phi,\Omega_H)\ , \tag{B4}$$

where

$$\Omega_H\equiv\omega\tau_H \tag{B5}$$

and

$$\tau_H\equiv\tau_a\exp(x_s)\equiv\tau_a r\ . \tag{B6}$$

Here ϕ is a parameter different from but related to the slope of the log-log frequency response.[7,9,15] For a class-I conductive system without a glass transition, one finds that $\phi=1-bT$, where b is independent of temperature. The unnormalized EDTR response at the impedance level is given by

$$Z=R_\infty+(R_0-R_\infty)A(x_s,\phi,\Omega_H)\ , \tag{B7}$$

where EDTR identifying subscripts have been omitted.

For the box distribution, $\phi=1$ for a conductive system and 0 for a dielectric one. Note, however, that in the usual temperature-independent-activation-energy case (class I), these values are attained[6,14] only at $T=0$. For these and some other integral and fractional values of ϕ, closed-form results may be found[5,7] from Eq. (B4). For $\phi=1$, Eq. (B7), written in normalized form, yields, for the EDTR$_1$,

$$Z_{bN}\equiv Z_b/R_{b0}$$

$$=R_{b\infty N}+[(1-R_{b\infty N})/(1-r^{-1})]$$

$$\times\ln[(1+i\Omega_H)/(1+i\Omega_H r^{-1})]/i\Omega_H\ , \tag{B8}$$

where $R_{b\infty N}\equiv R_{b\infty}/R_{b0}$ and $\tau_H r^{-1}\equiv\tau_L$, here equal to just τ_a. The subscript b identifies box-distribution results. As discussed in Appendix A, all dielectric effects have been subtracted here and in Eq. (B7). A slight generalization of a result of Dyre[2,3,8] for the present situation leads to

$$R_{b0}\equiv\epsilon_V/C_c\sigma_{b0}=(1-r^{-1})\tau_H/C_c x_s$$
$$=(\tau_a/C_c x_s)(r-1)\ . \tag{B9}$$

This expression approaches a virtually temperature-independent constant,

$$\zeta\equiv(\tau_a/C_c)=(C_c\Gamma_H)^{-1}\ , \tag{B10}$$

as $r\to 1$ ($T\to\infty$ with E_H finite or $E_H\to 0$ with $T\neq 0$). In deriving Eq. (B9), for simplicity the γ parameters of Ref. 3 have been identified, following Dyre,[3] as the Γ's that appear there and here. Now, if one assumes on the basis of one-dimensional calculations[3,4] that $\sigma_b'(\infty)/\epsilon_V=\langle\Gamma\rangle$, it follows that

$$R_{b\infty}=\zeta x_s/(1-r^{-1})\ , \tag{B11}$$

again equal to ζ for $x_s=0$. Thus, in this limit, one properly finds that $(R_{b0}-R_{b\infty})=0$. Finally, we can define C_{b0} as τ_H/R_{E0}.

Now in the limit of large r ($T\to 0$), the normalized EDTR$_1$ admittance may be expressed, when any $R_{b\infty}$ present is ignored, as the simple equation

$$Y_{bN}\equiv\sigma_b/\sigma_{b0}=i\Omega_H/\ln[1+i\Omega_H]\ , \tag{B12}$$

exactly the same in form as the PPA of Dyre[2] and also the same as the random-free-energy-barrier box-distribution model solved in the continuous-time random walk approximation for a hopping model.[3]

2. BEM and GBEM equations

Next, an EMA response function appropriate for $r\leq\infty$, the GBEM, will be derived, and a subscript E will be used to identify BEM and GBEM responses. Dyre obtained only a final response equation for this situation for the $r\to\infty$ limit.[3] The basic 3D EMA equation for the random free-energy model with a uniform distribution may be written in terms of $x_s\equiv\ln(r)$ as[3]

$$\exp[x_s/(1+\chi)]=(\Gamma_H+\chi\sigma_E/\epsilon_V)/(\Gamma_L+\chi\sigma_E/\epsilon_V)\ , \tag{B13}$$

where σ_E is the EMA complex conductivity and χ is given by

$$\chi\equiv(2+a)/(1-a)\ , \tag{B14}$$

with

$$a\equiv(\xi/3)(i\omega\epsilon_V/\sigma_{E0})/(\sigma_E/\sigma_{E0})\ . \tag{B15}$$

The dimensionless numerical constant ξ equals ≈ 0.253 and $\sigma_{E0}\equiv\sigma_E'(0)$. Define $\sigma_E/\sigma_{E0}\equiv Y_N$, termed Y_{EN} here. These equations are equivalent to those of Dyre[3] except that he used a first-order expansion in frequency of χ in his further developments of a $T\to 0$ equation, a path not appropriate for the present more general solution.

Now since $(1+\chi)^{-1}=(1-a)/3$, the left-hand side of Eq. (B13) may be written as $\exp[(x_s-i\Omega_E/Y_{EN})/3]$ with

$$\Omega_E\equiv\omega\tau_E \tag{B16}$$

and

$$\tau_E\equiv\xi\epsilon_V x_s/9\sigma_{E0}\equiv\xi C_c x_s R_{E0}/9\equiv R_{E0}C_{E0}\ , \tag{B17}$$

where τ_E is the effective relaxation time for the frequency response. It then follows that

$$C_{E0}/C_c\equiv\Delta C'(0)/C_c\equiv\epsilon_{E0}=\xi x_s/9\ . \tag{B18}$$

The above result for τ_E is similar to but more appropriate than that derived by Dyre[3] after further approximations, a result involving Γ_H rather than the present x_s. But in later work,[1,2] he derived by a different method an expression for τ_E similar to that here, when one sets his distribution function $p(E_g(0))$ to E_H^{-1}, as is indeed appropriate for the box distribution. His result is then larger than that here by a factor of $3\epsilon_\infty/\epsilon$. It follows from Eq. (B13) that

$$\sigma_{E0}=\epsilon_V\Gamma_H(1-r^{-2/3})/\{2(r^{1/3}-1)\}\equiv\epsilon_V/R_{E0}C_c\ , \tag{B19}$$

which approaches ϵ_V/τ_a for $r\to 1$ and

$$\epsilon_V\Gamma_H^{2/3}\Gamma_L^{1/3}/2=(\epsilon_V/2\tau_a)\exp(-x_s/3)$$

as r becomes large. Now we may write

$$R_{E0}=2\zeta(r^{1/3}-1)/(1-r^{-2/3})\ , \tag{B20}$$

equal to just ζ for $r\to 1$.

On solving Eq. (B13) for Y_{EN} and transforming to the normalized complex modulus M_{EN}, here defined as $i\Omega_E/Y_{EN}$, one finds the following implicit expression for M_{EN}:

$$M_{EN}=i\Omega_E\Big/\left\{\left[\frac{x_s-3M_{EN}}{x_s+3M_{EN}/2}\right]\times\left[\frac{1-\exp(-x_s/3)}{\exp(-M_{EN})-\exp(-x_s/3)}\right]\times\left[\frac{1-\exp(-2x_s/3-M_{EN})}{1-\exp(-2x_s/3)}\right]\right\}\ . \tag{B21}$$

This equation was not derived by Dyre and must be solved as a function of Ω_E for various values of x_s in order to investigate the approaches of M_{EN} and Y_{EN} to $T\to 0$ behavior.

The $T\to 0$ limiting form of Eq. (B21), obtained when $x_s\to\infty$, is

$$M_{EN}=i\Omega_E\exp(-M_{EN})=\ln(i\Omega_E/M_{EN}) \tag{B22}$$

or

$$Y_{EN}=i\Omega_E/\ln(Y_{EN})=\exp(i\Omega_E/Y_{EN})\ . \tag{B23}$$

Equation (B23), the BEM equation, was apparently first derived by Bryksin[14] and is the only form used by Dyre[1-3] (But with a less appropriate definition for τ_E for the present situation[3]). It is clear that since $\tau_E \rightarrow \infty$ as $r \rightarrow \infty$, the actual $r = \infty$ limit is meaningless since for a fixed value of Ω_E, say, Ω_{EF}, the corresponding $\omega_F = \Omega_{EF}/\tau_E$ approaches zero as $\tau_E \rightarrow \infty$ for any finite value of Ω_{EF}. For specified values of Ω_E and x_s, one may readily solve any of these implicit equations for their complex roots to high accuracy using the MATHEMATICA system.[35]

Since it is convenient to use Ω_E as the normalized frequency variable for comparison of the predictions of the GBEM and EDTR equations, we must replace Ω_H in Eqs. (B43), (B7), (B8), and (B12) by its equivalent $\Lambda\Omega_E$, where the scaling factor $\Lambda \equiv \tau_H/\tau_E$. For comparison purposes, let us replace E_H in τ_H by $E_H/3$, as discussed in Sec. III B. Then the above results allow us to write a theoretical expression for Λ, say, Λ_t, as

$$\Lambda_t = (2\epsilon_{E0})^{-1}(1-r^{-2/3})/(1-r^{-1/3}) , \tag{B24}$$

which approaches $(2\epsilon_{E0})^{-1}$ for large r, a temperature-dependent quantity. For $x_s = 40$, $\Lambda_t \simeq 3.4$.

Now Dyre[2,3] has used a value of Λ of 2, said to be derived from comparison of the first-order Taylor expansions of Y_{bN} and Y_{EN} as $\omega \rightarrow 0$ and $r \rightarrow \infty$. In these limits, however, the MacLaurin series expressions show that $(Y'_{XN}-1)$ approaches $(\omega\tau_H)^2/12$ for the EDTR$_1$ and $(\omega\tau_E)^2/2$ for the BEM. Thus agreement requires $\Lambda \simeq 2.45$. But both equations lead to a limiting value of $(\omega\tau_X)$ for Y''_{XN}, requiring $\Lambda = 1$. Since both relations cannot be simultaneously satisfied, for the present comparisons proportional-weighting CNLS fitting of the EDTR equation to both real and imaginary Y_{EN} data points simultaneously was carried out with Λ taken as a free fitting parameter. Its estimated value, depending on the particular type of fitting employed, was generally found to satisfy $1 < \Lambda < 2$.

For $r \gg 1$, the above results lead to

$$R_{E0} \rightarrow 2r^{1/3}\xi = 2r^{1/3}R_{E\infty} \tag{B25}$$

and

$$\tau_E \equiv R_{E0}C_{E0} \rightarrow 2\xi x_s r^{1/3}\tau_a/3 . \tag{B26}$$

For this model, $R_{E\infty}$ takes the simple form

$$R_{E\infty} \equiv R_{E0}R_{E\infty N} = \xi . \tag{B27}$$

The present normalization leads to

$$C_{XN} \equiv C_X/C_{E0} \equiv \epsilon_{XN} \equiv \epsilon_X/\epsilon_{E0} , \tag{B28}$$

where

$$\epsilon_X = C_X/C_c . \tag{B29}$$

But it turns out from the numerical results that $C_{E0N} \equiv C_{E0}/C_{EN}$ is not generally unity, but approaches it only as $T \rightarrow 0$, since we find that for $x_S \geq 20$, $C_{E0N} \simeq 1 - 4.5x_s^{-1}$, probably equal within numerical uncertainty to the EDTR ϕ expression discussed in Sec. III B and, if so, the source of such a response found when fitting the GBEM with the EDTR model.

The GBEM and BEM are not unique in that they each have an infinity of complex roots. This was discovered for the GBEM by using contour plots in the complex plane to show root positions. Thompson then pointed out[36] that if one added the term $2\pi ni$ (n an integer) to the $\ln(Y_{EN})$ term in Eq. (B23) to account for the infinite number of sheets of the logarithm function in the complex plane, a new root appears for each n value, one which satisfies the exponential form of the BEM shown in Eq. (B23) as well. Luckily, the $n \neq 0$ roots seem to be nonphysical since they lead to a change in sign of Y'' from positive to negative over all or part of the frequency range.

[1] J. C. Dyre, Phys. Rev. B **47**, 9128 (1993).
[2] J. C. Dyre, Phys. Rev. B **48**, 12 511 (1993).
[3] J. C. Dyre, J. Appl. Phys. **64**, 2456 (1988). The present ratio Λ is misprinted in this work as 0.5 instead of 2.
[4] H. Frohlich, *Theory of Dielectrics* (Clarendon, Oxford, 1949), p. 93.
[5] A. Matsumoto and K. Higasi, J. Chem. Phys. **36**, 1776 (1962).
[6] J. R. Macdonald, J. Appl. Phys. **34**, 538 (1963).
[7] J. R. Macdonald, J. Appl. Phys. **58**, 1955 (1985).
[8] J. C. Dyre, Phys. Lett. **108A**, 457 (1985).
[9] J. R. Macdonald, J. Appl. Phys. **65**, 4845 (1989).
[10] G. A. Niklasson, J. Appl. Phys. **66**, 4350 (1989).
[11] J. R. Macdonald, J. Appl. Phys. **61**, 700 (1987).
[12] J. W. Haus and K. W. Kehr, Phys. Rep. **150**, 263 (1987).
[13] M. P. J. van Staveren, H. B. Brom, and I. J. de Jongh, Phys. Rep. **208**, 1 (1991).
[14] V. V. Bryksin, Fiz. Tverd. Tela (Leningrad) **22**, 2441 (1980) [Sov. Phys. Solid State **22**, 1421 (1980)].
[15] J. R. Macdonald and J. C. Wang, Solid State Ion. **60**, 319 (1993).
[16] J. R. Macdonald, J. Appl. Phys. **75**, 1059 (1994).
[17] *Impedance Spectroscopy—Emphasizing Solid Materials and Systems,* edited by J. R. Macdonald (Wiley-Interscience, New York, 1987).
[18] J. R. Macdonald and L. D. Potter, Jr., Solid State Ion. **23**, 61 (1987). The LEVM program, V.6, is comprehensive and includes many powerful features for accurate fitting of conductive- and dielectric-system frequency and time response data. In the present work, proportional data weighting was used for all LEVM fits.
[19] J. R. Macdonald, Electrochim. Acta **35**, 1483 (1990).
[20] W. K. Lee, J. F. Liu, and A. S. Nowick, Phys. Rev. Lett. **67**, 1559 (1991).
[21] I. I. Fishchuk, Phys. Status Solidi A **93**, 675 (1986).
[22] H. D. Woltring, Adv. Eng. Software **8**, 104 (1986).
[23] R. H. Cole and E. Tombari, J. Non-Cryst. Solids **131-133**, 969 (1991).
[24] D. W. Davidson and R. H. Cole, J. Chem. Phys. **19**, 1484 (1951).
[25] E. N. Economou, *Green's Functions in Quantum Physics*

(Springer, Berlin, 1983); see Eq. (5.52).
[26]J. R. Macdonald and M. K. Brachman, Rev. Mod. Phys. **28**, 393 (1956).
[27]J. H. Ambrus, C. T. Moynihan, and P. B. Macedo, J. Phys. Chem. **76**, 3287 (1972).
[28]B. Gross, J. Appl. Phys. **57**, 2331 (1985).
[29]U. Strom, Solid State Ion. **8**, 255 (1983).
[30]C. A. Angel, Chem. Rev. **90**, 523 (1990).
[31]K. Funke, Prog. Solid State Chem. **22**, 111 (1993).
[32]F. S. Howell, R. A. Bose, P. B. Macedo, and C. T. Moynihan, J. Phys. Chem. **78**, 639 (1974).
[33]S. K. Jain, K. Pathmanathan, and G. P. Johari, Phys. Chem. Glasses **29**, 198 (1988).
[34]S. Alexander, J. Bernasconi, W. R. Schneider, and R. Orbach, Rev. Mod. Phys. **53**, 175 (1981).
[35]S. Wolfram, *Mathematica: A System for Doing Mathematics by Computer,* 2nd ed. (Addison-Wesley, Redwood City, California, 1991).
[36]W. J. Thompson (private communication).